Elastoplastic finite element modeling of a deep-drawing manufacturing process in Abaqus

Jackson Sammartino

April 23, 2025

***Abstract* — Finite element analysis was performed, using Abaqus software, on a 3D model to simulate a deep-drawing manufacturing process of a thin sheet metal part ("blank"). This problem involved elastoplasticity, isotropic hardening, and large deformation. Simulation steps included application of a binder force (8800 N or 1250 N), a downward punch stroke of 70 mm, and removal of tooling to simulate springback. 3D solid elements did not converge, but 3D shell elements yielded useful results regarding the stresses experienced during each Step, approximate springback, effective plastic strain, and change in thickness of the blank. Results for the lower binder force made physical sense, showing lower stress/strain and less deformation.**

***Index Terms* — Abaqus software, deep-drawing simulation, elastoplastic modeling, nonlinear finite element analysis.**

I. Introduction

The goal of this project was to model the deep-drawing manufacturing process of an elastoplastic metal material under various conditions. Figure 1 depicts a planar view of this process, where a thin sheet of material, referred to as the "blank," is clamped between the blank holder and the die using some "binder force," while the punch moves downward to form the blank into a cup-like shape. Then, the tooling and loads are removed, resulting in "springback" of the blank as elastic energy is released. Note that due to symmetry about the vertical centerline, this process can be modeled using just half of the geometry (Fig. 2) to reduce computational cost.

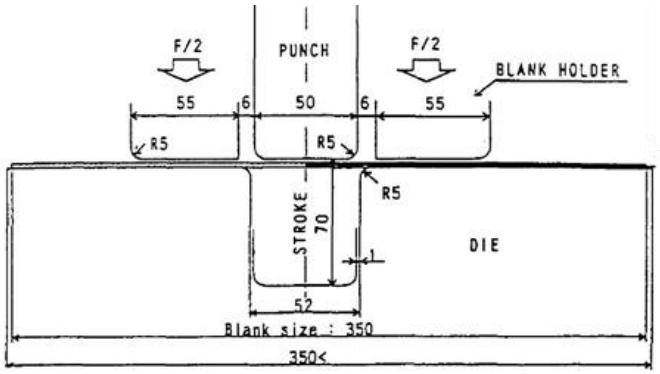

Fig. 1: Planar view of deep-drawing manufacturing process showing punch, blank, blank holder, and die components [1]. Units are in mm.

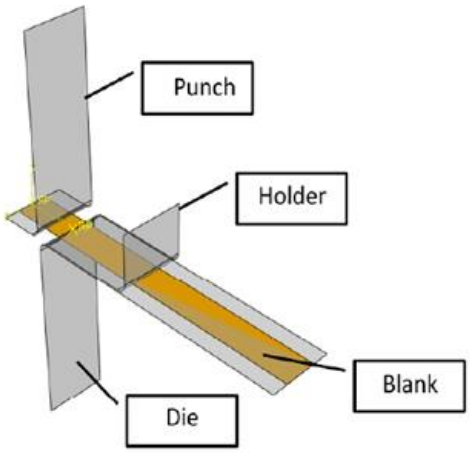

Fig. 2: Isometric view of the effective model, only requiring half of the geometry due to symmetry [1].

Most common engineering metals are elastoplastic- they behave elastically up to a certain yield stress, then plastically deform beyond that point. This transition poses challenges for several reasons. Firstly, stress is only a function of elastic strain, meaning that plastic (or permanent) strain must be isolated and subtracted off from total strain [2]. This implies that under certain combinations of loading and unloading, the same stress can exist for different values of strain (non-potential relationship). Thus, *hypoelastic* relations are usually given in terms of stress and strain *rates* [2]. Additionally, when the yield stress of a material is exceeded, hardening occurs, whereby the yield strength increases for subsequent loadings. Two hardening models- kinematic and isotropic, as well as a combined model- can be used for return mapping to the yield surface [2]. Lastly, this problem in particular involves large deformation of the metal blank, meaning that an objective, coordinate-independent formulation must be used [2]. With these characteristics in mind, it is clear that analyzing elastoplastic problems is much more complicated than studying traditional linear elastic materials, which is why finite element modeling software like Abaqus is invaluable.

Abaqus was used in this project to model the deep-drawing process under different conditions. Two different binder forces of 8800 N and 1250 N were tested, for both 3D solid elements and shell elements.

II. Procedure

Problem Geometry and Material Properties

Four Parts were created in Abaqus (Fig. 3) and dimensioned relative to one another according to Figure 1. The blank Part was created as a 3D deformable solid, or as a shell, with length 175 mm, depth 17.5 mm, and thickness 0.78 mm. The punch, blank holder, and die were modeled as 3D analytical rigid Parts, extruded an arbitrary depth of 50 mm (so long as they covered the blank Part). Reference points for each of these rigid Parts were created to apply boundary conditions.

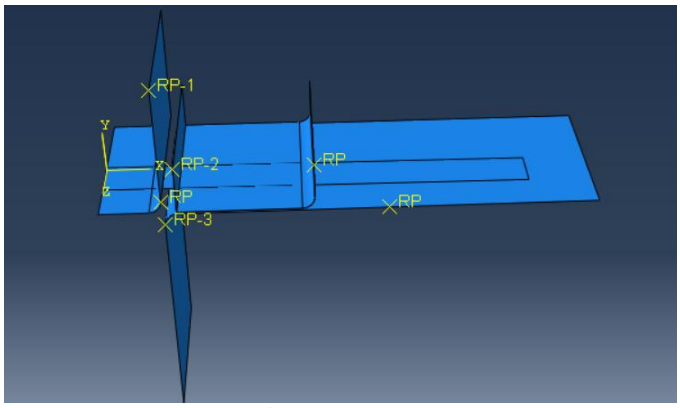

Fig. 3: Abaqus Assembly of the deep-drawing model. Note that the blank Part is 17.5 mm in depth while the other Parts are an arbitrary greater depth.

Material properties of the blank Part, shown in Table I below, were input into Abaqus [1]. The plastic modulus H was effectively implemented as the slope of the yield stress-strain plastic data points. Pure isotropic hardening was used. The friction coefficient μ was defined in an general contact Interaction between all surfaces. Various meshes were tested, discussed in the following section III. All elements were created of unit depth 17.5 mm for simplicity.

Table I: Material Properties of Blank Part

Property	Symbol	Value
Elastic modulus	E	206 MPa
Poisson's ratio	v	0.3
Initial yield stress	σ_y	167 MPa
Plastic modulus	H	10 GPa
Friction coefficient	μ	0.14

Simulation Steps

Due to the complexity of this problem, Steps were created with the nonlinear geometry feature on, 1500 increments allowed per step, initial/minimum/maximum increments of $0.01/10^{-9}/0.1$, and automatic stabilization (default settings for dissipated energy fraction). Boundary conditions were carefully implemented during each Step. For the Initial Step, the die Part was fully fixed, while the blank holder and punch Parts were only free to move in the U2 direction. The free end of the blank Part (right-hand side of Fig. 3) was fixed in the U2 and U3 directions to maintain contact with the die and prevent undesired rigid body motion. Finally, an x-symmetry boundary condition was applied to the clamped end of the blank Part (left-hand side of Fig. 3).

In the BinderForce Step, a Load was placed on the blank holder Part reference point, equal to half of the binder force, in the negative U2 direction. All other boundary conditions were propagated from the Initial Step.

In the PunchDown Step, a displacement of -70 mm was applied to the punch Part reference point. All other boundary conditions, including the binder force Load, were propagated.

Lastly, in the SpringBack Step, many changes were made to simulate removal of the tooling from the blank Part. The binder force Load was set to zero, and the blank holder and punch Parts were displaced to 50 mm in the U2 direction. The die Part was displaced to 200 mm in the negative U2 direction. The x-symmetry and fixed-U3 boundary conditions for the blank Part were propagated, but the fixed-U2 constraint was removed to allow for springback. This sequence of steps accurately models the entire deep-drawing process.

III. Results and Discussion

Meshing and Convergence

Although a variety of simulation settings were attempted, no convergence was observed for 3D solid elements (discussed in the last section). For the shell elements, a mesh convergence analysis was performed to determine the most accurate results. Table II summarizes this process and identifies the ideal mesh density for convergence of maximum stress values, at different Steps of the simulation.

Table II: Mesh Stress Convergence for Blank Part (Shell)

Elements	BinderForce	PunchDown	SpringBack
20	*Did*	*Not*	*Converge*
30	19.29	214.2	195.0
40	21.93	218.5	220.0
50	**23.64**	**267.1**	**220.6**
60	*Did*	*Not*	*Converge*
55	*Did*	*Not*	*Converge*

Note: Values are von Mises stresses (MPa) at each Step of the simulation. This mesh convergence process was performed for the shell element model with 8800 N binder force, and applied to subsequent trials.

Deformed Shape Plots

The following Figures 4-5 show the blank Part's deformation under specified conditions, before and after springback.

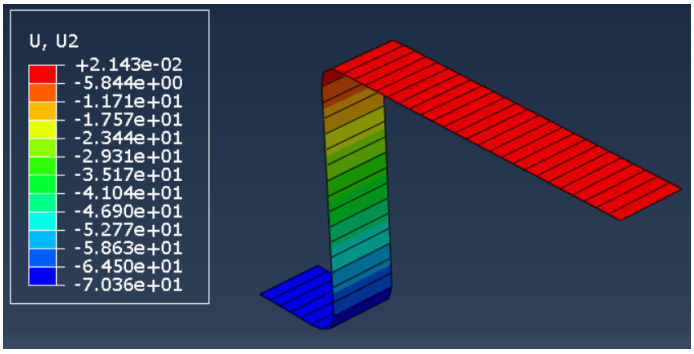

Fig. 4: Deformed blank Part (shell), 8800 N binder force, before springback.

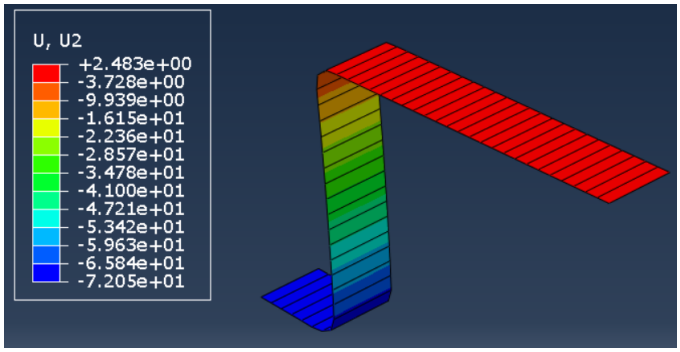

Fig. 5: Deformed blank Part (shell), 8800 N binder force, after springback.

These two plots indicate that the top horizontal region of the blank sprung upwards by about 2.5 mm after removal of the tooling, while the rest of the Part experienced ~1 mm of springback. The ratios of these quantities makes sense considering the Part geometry, but springback values were expected to be about one order of magnitude higher. This discrepancy may have resulted from modeling only half of the blank Part due to symmetry, or from the order/direction in which the tooling (die, blank holder, and punch) Parts were removed.

Contour Plot of Effective Plastic Strain

The following Figure 6 shows the effective plastic strain within the blank Part under specified conditions. These results show that large plastic deformation occurred as the blank Part was drawn into the cavity along the sides of the die Part. No plastic strain was observed along the regions that remained horizontal, implying that their deformation was small and never reached the yielding point.

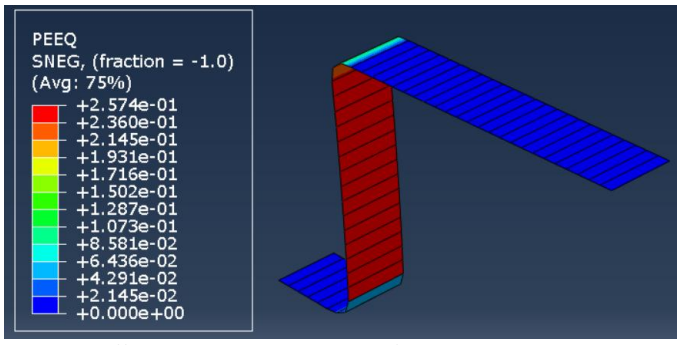

Fig. 6: Effective plastic strain contour of the blank Part (shell), 8800 N binder force, after springback.

Thickness Variation along Blank Part

Section thickness (STH) was added to the Field Output Request to observe how the thickness of the elements deviated from the initial 0.78 mm (Figure 7). In agreement with the plot of plastic strain (Fig. 6), the thickness only changed (decreased) along the vertical region as the metal was stretched significantly against the die wall.

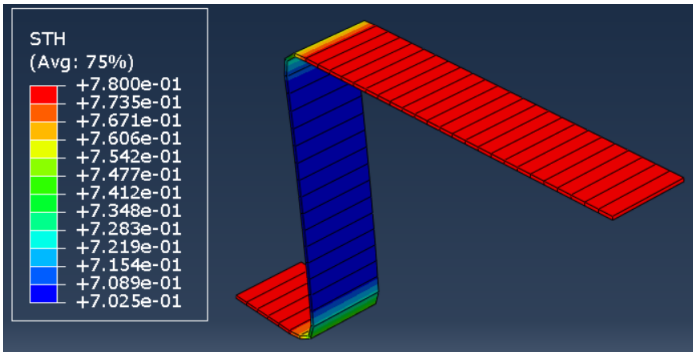

Fig. 7: Thickness variation (mm) of the blank Part (shell), 8800 N binder force, after springback.

Comparison of Binder Forces

While the 8800 N binder force produced reliable results, the 1250 N binder force did not converge, even when the incrementation values were relaxed. It was determined that a 1250 N binder force was insufficient for deep-drawing because it allowed the blank to push the blank holder out of the way and/or slide out of the tooling fixture. Instead, a 2000 N binder force was tested, converged, and the .cae was saved (Appendix). The results were compared to the 8800 N binder force simulation, as shown in Tables III-IV below.

Table III: Binder Force Max Stress Comparison

Quantity	BinderForce	PunchDown	SpringBack
8800 N	23.64	267.1	220.6
2000 N	6.914	239.7	235.5

Note: Values are von Mises stresses (MPa) at each Step of the simulation.

Table IV: Binder Force Max Deformation Comparison

Quantity	Approximate Springback	Equivalent Plastic Strain	Minimum Thickness
8800 N	2.462 mm	0.2574	0.7025 mm
2000 N	2.273 mm	0.1816	0.7448 mm

These differences make physical sense. A lower binder force generally led to lower stresses (Table III), and less deformation, as evidenced by the lower plastic strain and less change in thickness compared to the nominal 0.78 mm (Table IV).

Comparison of Shell to Solid Elements

The greatest limitation of this project was the inability to model the deep-drawing process using 3D solid elements for comparison to 3D shell elements. Attempts were made to make solid elements converge, including: using anywhere from 1 to 5 elements in the thickness direction to model bending, greatly relaxing the incrementation constraints, using different stabilization methods, and using different methods of integration.

Some reasons why convergence was not obtained may be: element locking on the sharp bend radius as the blank Part flows into the die cavity, penetration and/or overclosure between the multiple contacting surfaces, and using purely isotropic hardening instead of a combined model. Still, significant and useful simulation results were obtained with shell elements.

APPENDIX

Abaqus .cae Files

A supplemental .cae file of the deep-drawing simulation (shell elements, 2000 N binder force) was attached to the project submission.

REFERENCES

[1] Kim, Nam-Ho, “Project 2,” assignment description, course EGM6352, University of Florida, Spring 2025.
[2] Kim, Nam-Ho, “Chapter 4: FEA for Elastoplastic Problems,” class notes, course EGM6352, University of Florida, Spring 2025.